nature structural & molecular biology

SUPPLEMENTARY INFORMATION

https://doi.org/10.1038/s41594-017-0009-1

In the format provided by the authors and unedited.

Structural basis of TRPV5 channel inhibition by econazole revealed by cryo-EM

Taylor E. T. Hughes[1], David T. Lodowski[1,2], Kevin W. Huynh[1,3], Aysenur Yazici[4], John Del Rosario[4], Abhijeet Kapoor[5], Sandip Basak[6], Amrita Samanta[1,6], Xu Han[1], Sudha Chakrapani[6], Z. Hong Zhou[3], Marta Filizola[5], Tibor Rohacs[4], Seungil Han[7] and Vera Y. Moiseenkova-Bell[1,6,8]*

[1]Department of Pharmacology, School of Medicine, Case Western Reserve University, Cleveland, OH, USA. [2]Department of Nutrition, School of Medicine, Case Western Reserve University, Cleveland, OH, USA. [3]California NanoSystems Institute, University of California, Los Angeles, Los Angeles, CA, USA. [4]Department of Pharmacology, Physiology and Neuroscience, New Jersey Medical School, Rutgers University, Newark, NJ, USA. [5]Department of Pharmacological Sciences, Icahn School of Medicine at Mount Sinai, New York, NY, USA. [6]Department of Physiology and Biophysics School of Medicine, Case Western Reserve University, Cleveland, OH, USA. [7]Pfizer Research and Development, Groton, CT, USA. Present address: [8]Department of Systems Pharmacology and Translational Therapeutics, Perelman School of Medicine, University of Pennsylvania, Philadelphia, PA, USA.
*e-mail: vmb@pennmedicine.upenn.edu

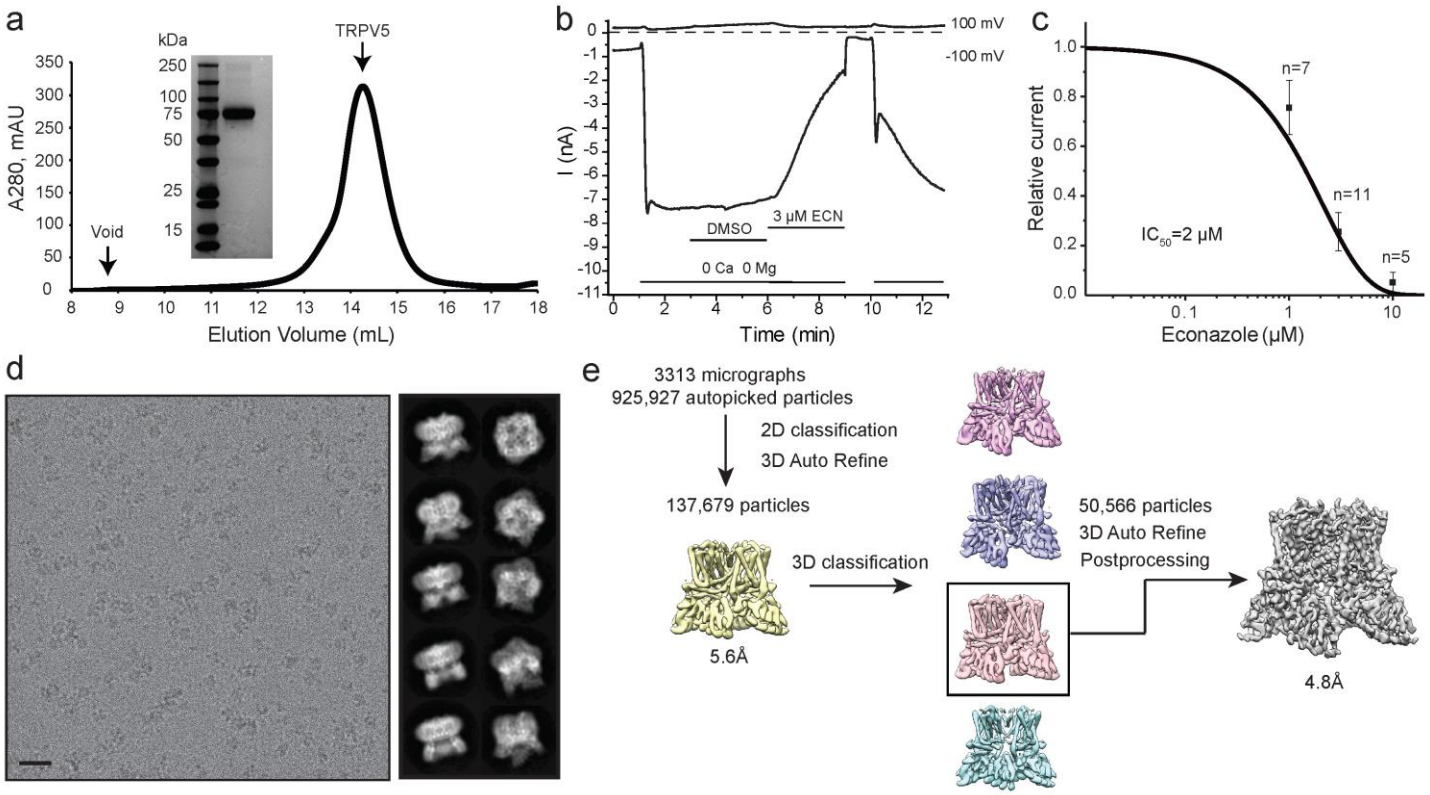

Supplementary Figure 1

TRPV5 purification, whole-cell electrophysiology, and data processing.

(**a**) A size exclusion chromatogram of purified TRPV5. The inset panel depicts a SDS-PAGE image of purified TRPV5. (**b**) Whole cell patch clamp experiments were performed as described in the methods section in HEK293 cells transfected with rbTRPV5 using a ramp protocol from -100 to 100 mV; currents are plotted at -100 and 100 mV, zero current is indicated by the dashed line. Representative trace (n=11), monovalent currents were initiated by removal of extracellular Ca^{2+} and Mg^{2+} and the application of 0.33 % DMSO and 3 μM econazole is indicted by the horizontal lines. (**c**) Concentration response curve for econazole. Error bars represent ± s.e.m. of the respective *n* biological replicates. (**d**) The first panel is a representative micrograph of TRPV5 incubated with econazole frozen in vitreous ice (n=3,313). Scale bar = 25 nm. The second panel depicts 2D class averages used when reconstructing the $TRPV5_{ECN}$ structure. (**e**) The workflow used to reconstruct $TRPV5_{ECN}$ to 4.8Å. A box around a 3D class indicates that that class was taken for further processing.

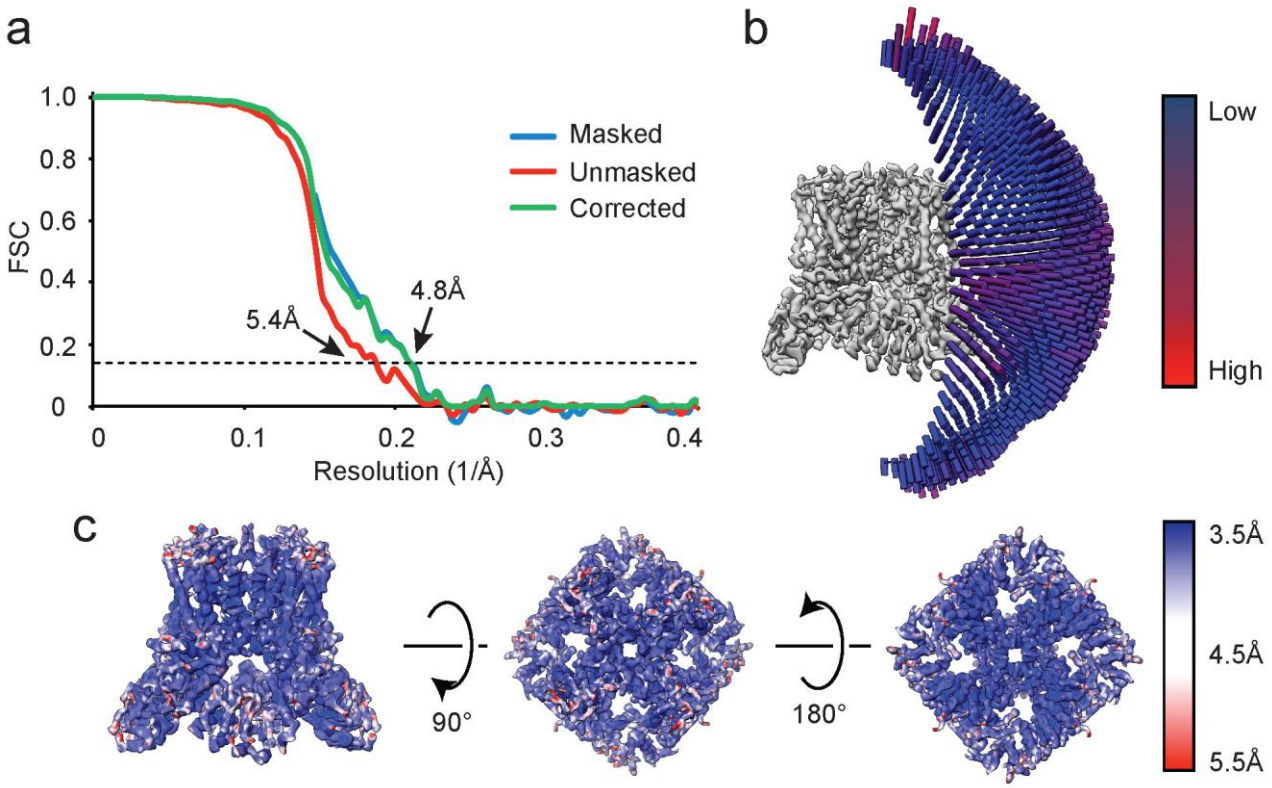

Supplementary Figure 2

Resolution data for $TRPV5_{ECN}$ refinement.

(**a**) FSC curves for masked, unmasked and corrected reconstructions. The dashed line represents an FSC of 0.143. (**b**) The angular distribution of 2D views for the final particles used for the reconstruction. High numbers of particles are represented as taller red cylinders while views with a low number of particles are shown as shorter blue cylinders. The final density map of $TRPV5_{ECN}$ is shown in grey. (**c**) Multiple views of the local resolution map of $TRPV5_{ECN}$. Local resolution was determined using ResMap software.

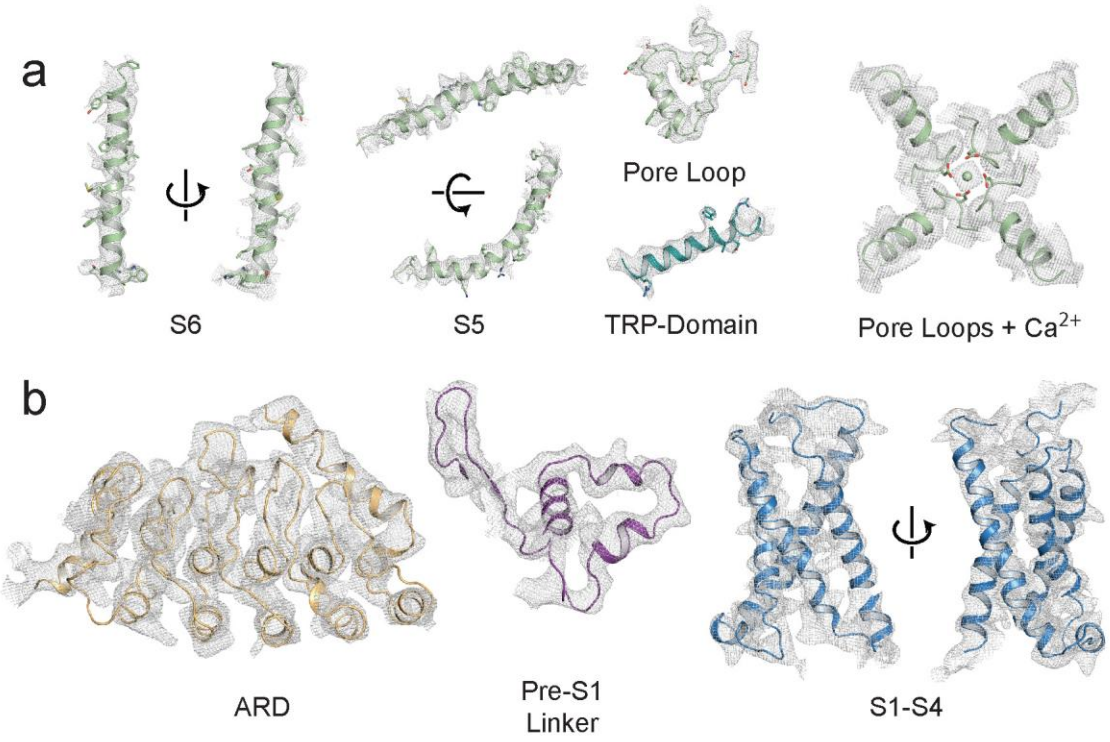

Supplementary Figure 3

TRPV5 model validation.

(**a**) Various helices of the $TRPV5_{ECN}$ model (cartoon) overlaid with the $TRPV5_{ECN}$ density map (mesh). Select residues are shown as sticks to illustrate the accuracy of the model. All helices shown are within the 3.5-4.0Å region of the structure. (**b**) Other domains of the $TRPV5_{ECN}$ model (cartoon) overlaid with the final $TRPV5_{ECN}$ density map (mesh). The different regions of the $TRPV5_{ECN}$ model are colored based on the diagram in Fig. 1b.

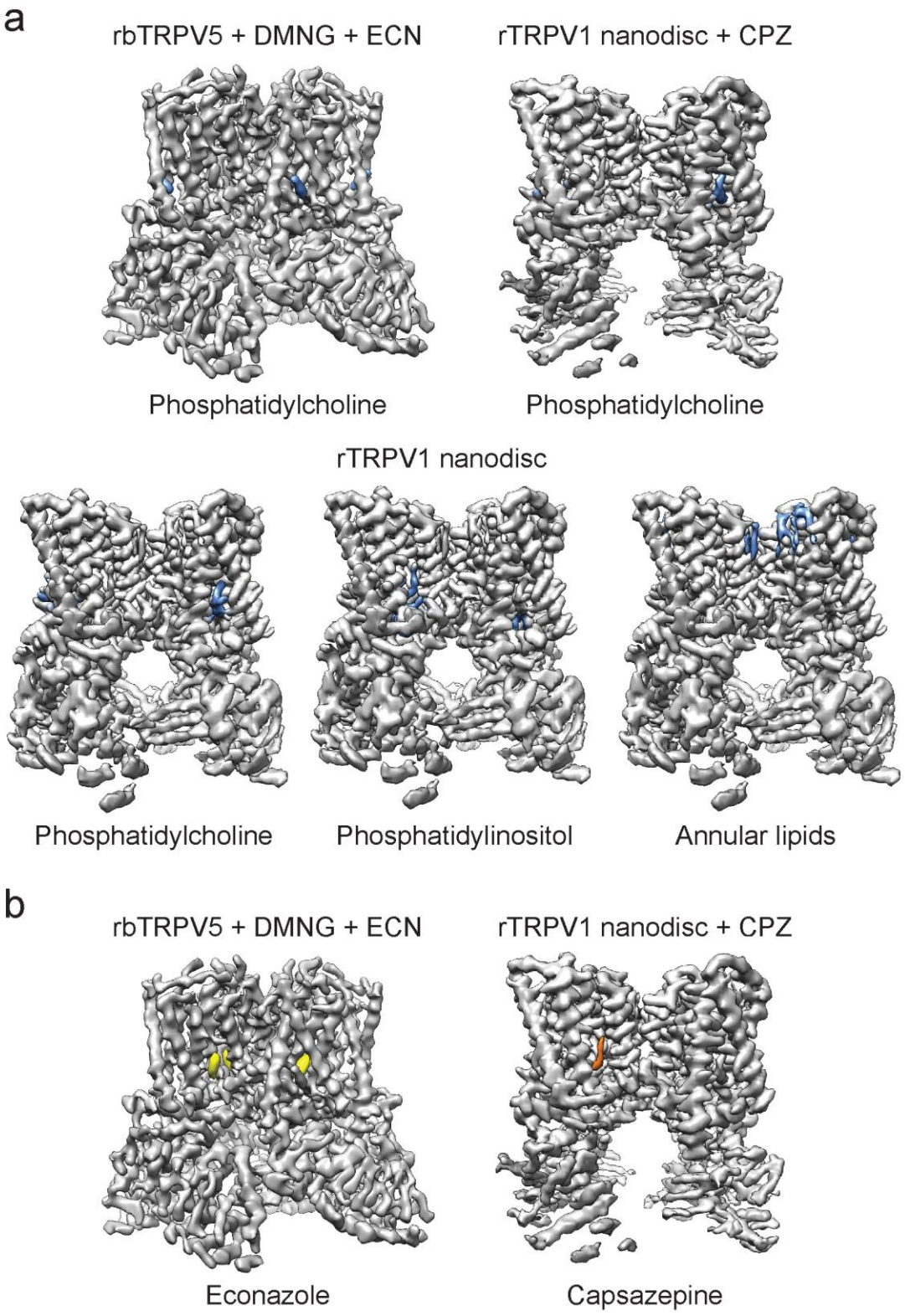

Supplementary Figure 4

Binding sites among TRPV subfamily members.

(**a**) Density maps of econazole (ECN) bound rabbit TRPV5, capsazepine (CPZ) bound rat TRPV1 solved in nanodiscs and apo rat TRPV1 solved in nanodiscs. Densities attributed to lipids in each structure are colored in blue. The lipid to which each density was ascribed is listed below each structure. (**b**) Density maps of econazole (ECN) bound rabbit TRPV5, capsazepine (CPZ) bound rat TRPV1 solved in nanodiscs. ECN densities are shown in yellow. Capsazepine densities are shown in orange.

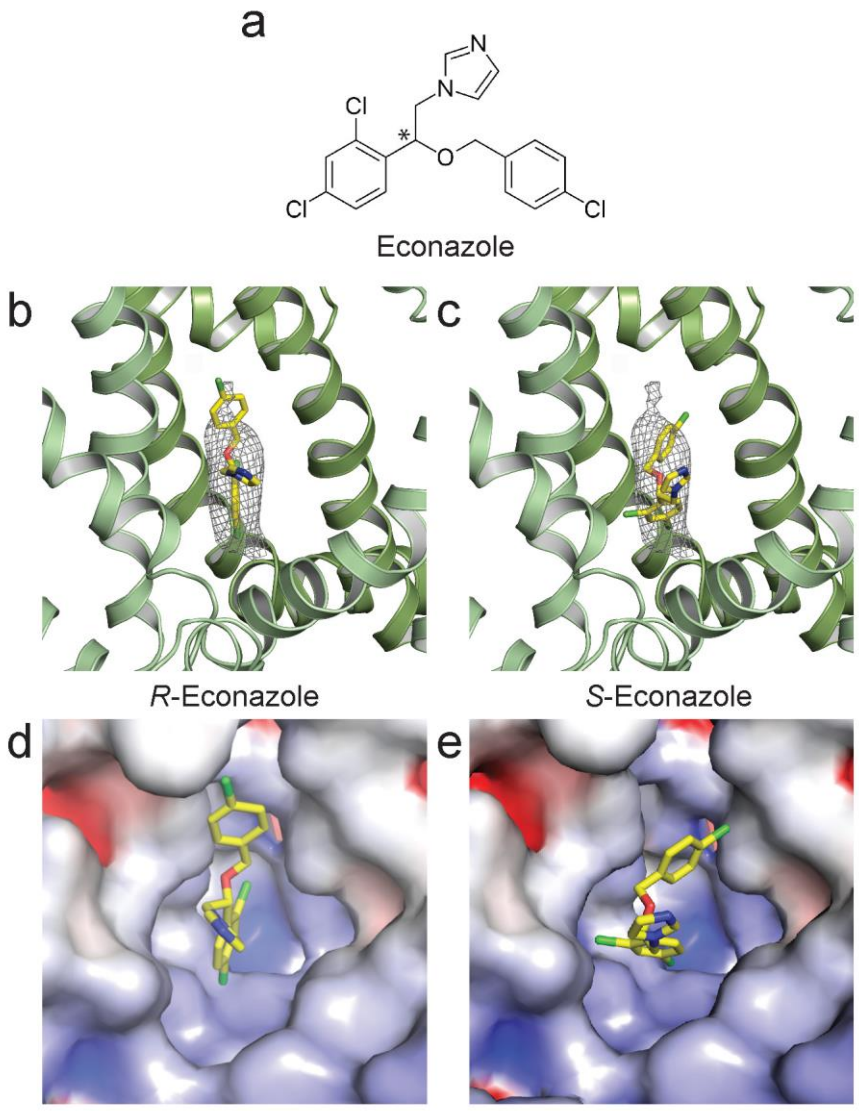

Supplementary Figure 5

Econazole-binding pocket.

(**a**) Molecular structure of econazole. The asterisk indicates the location of a chiral center. (**b**) Zoomed in view of the econazole binding pocket manually fitted with R-econazole (yellow). The grey mesh represents the cryo-EM density attributed to econazole. (**c**) Zoomed in view of the econazole binding pocket manually fitted with S-econazole (yellow). The grey mesh represents the cryo-EM density attributed to econazole. (**d-e**) An electrostatic map of $TRPV5_{ECN}$ was calculated via APBS software. The zoomed views depict the econazole binding pocket with R-econazole or S-econazole shown in yellow.

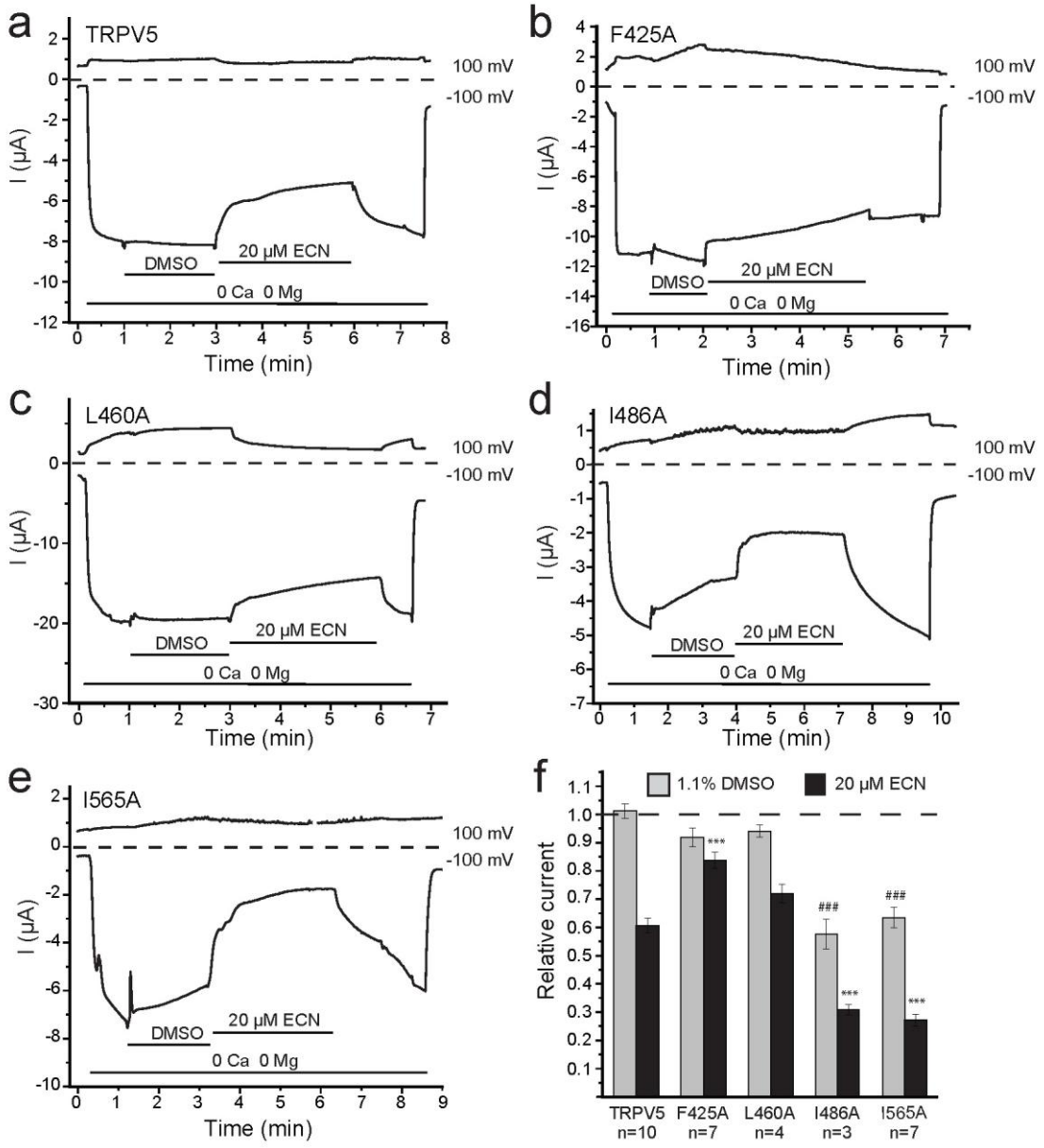

Supplementary Figure 6

Econazole effect on mutant TRPV5.

Two electrode voltage clamp (TEVC) experiments were performed similar to that described in Figure 2 on Xenopus laevis oocytes injected with cRNA encoding the wild type or various mutants of rabbit TRPV5. (**a-e**) Representative traces for WT and various TRPV5 mutants (n=10, n=7, n=4, n=3, n=7, respectively), currents are shown at -100 and +100 mV, zero current is indicated by the dashed line, the applications of 2.2 % DMSO (solvent) and 20 µM Econazole (ECN) are indicated by the horizontal lines. (**f**) Summary of the effects of 20 µM econazole and 2.2 % DMSO. *** p<0.001 indicates a difference between econazole inhibition in WT (first black column). ##p<0.01, ###p<0.001 indicates a difference from the effect of DMSO on WT channels (first

grey column); one way analysis of variance with Bonferroni post hoc comparison. Error bars represent ± s.e.m. of the respective *n* biological replicates.

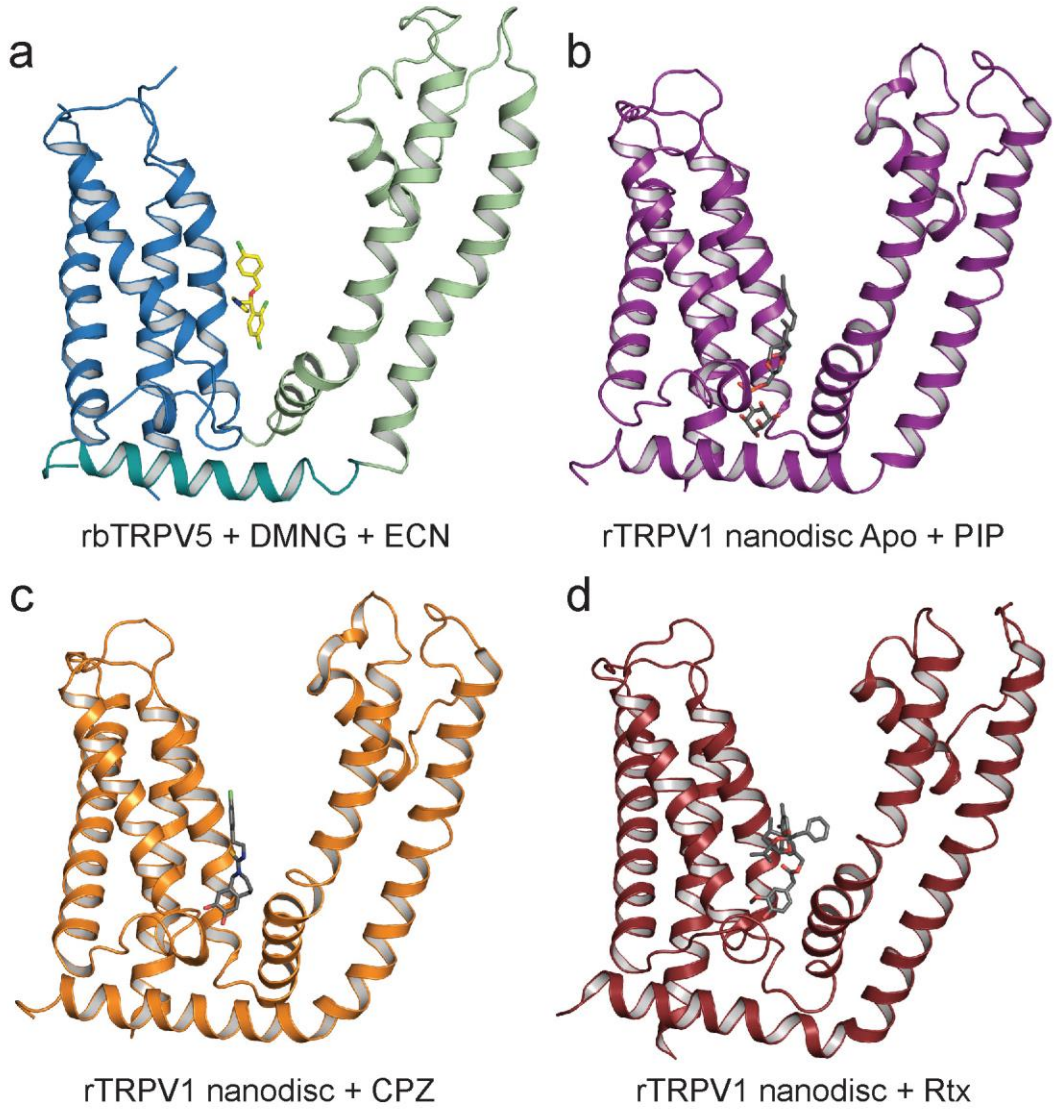

Supplementary Figure 7

Comparison of ligand binding pockets within the TRPV subfamily.

(**a**) The transmembrane domain (TMD) of $TRPV5_{ECN}$. Bound econazole (ECN) is represented as yellow sticks. The regions of $TRPV5_{ECN}$ are colored based on the diagram in Fig. 1b. (**b**) The TMD of rat TRPV1 solved in nanodiscs in the absence of added ligand (purple, PDB: 5IRZ). Bound phosphatidylinositol, a lipid cofactor of TRPV1, is shown in grey sticks. (**c**) The TMD of rat TRPV1 solved in nanodiscs in the presence of the inhibitor capsazepine (orange, PDB: 5IS0). The capsazepine molecule (CPZ) is shown in grey. (**d**) The TMD of rat TRPV1 solved in nanodiscs in the presence of the potent agonists, resiniferatoxin (RTX) and double-knot toxin (DkTx) is shown in red (PDB: 5IRX). The pocket depicted coordinates an RTX molecule (grey).

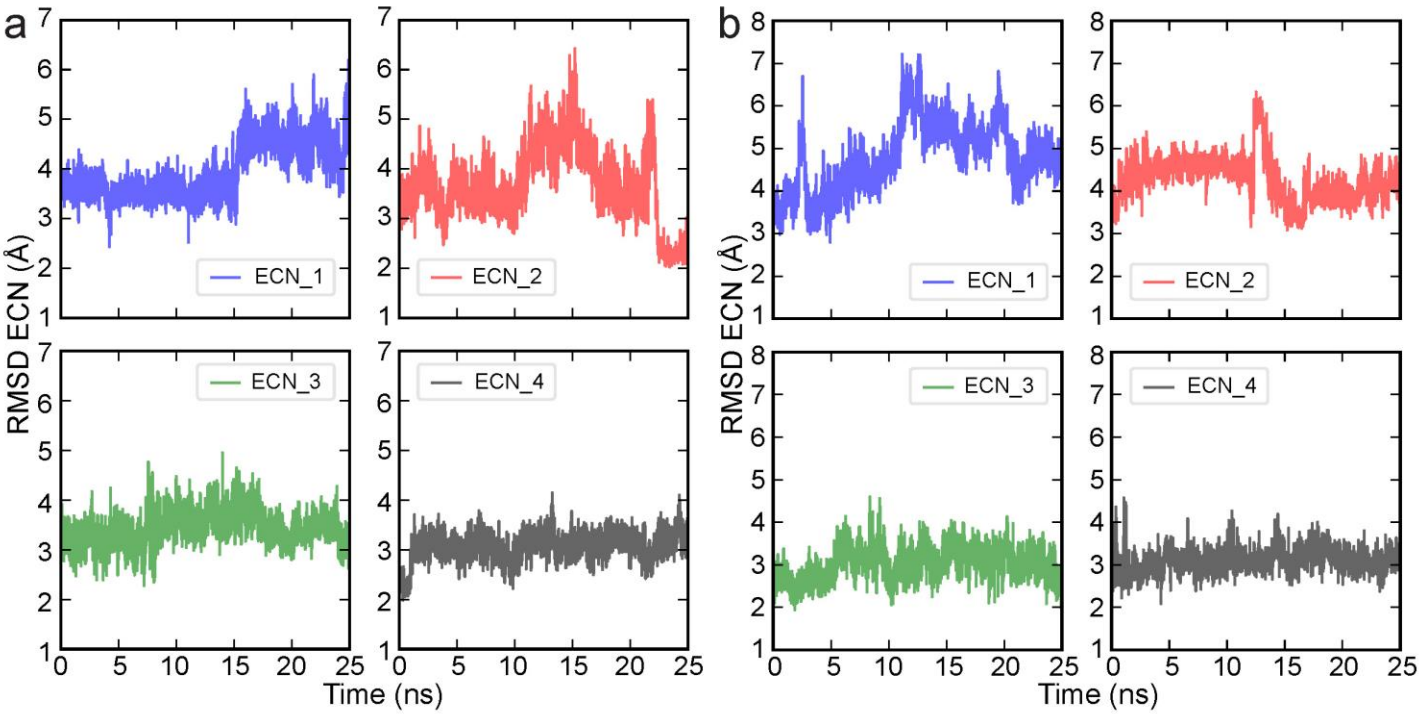

Supplementary Figure 8

Econazole flexibility during MD production run.

(**a**) Time evolution of the RMSD of R-econazole (labeled ECN_1 to ECN_4) with respect to the initial manual docking into the assigned electron density within the four monomers of TRPV5 (monomers A to D, respectively) during the 25 ns production run. (**b**) Time evolution of the RMSD of S-econazole (labeled ECN_1 to ECN_4) with respect to the initial manual docking into the assigned electron density within the four monomers of TRPV5 (monomers A to D, respectively) during the 25 ns production run.

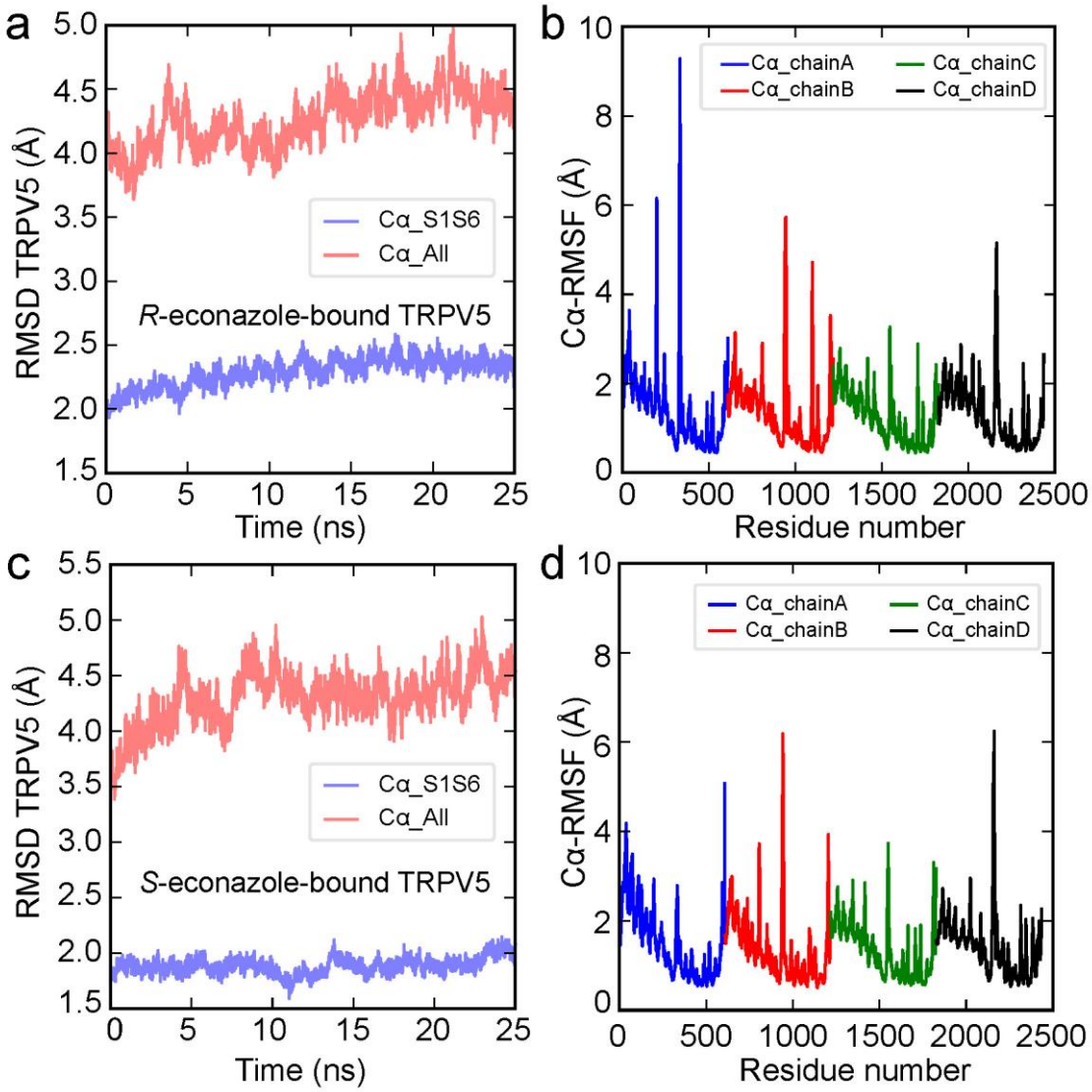

Supplementary Figure 9

TRPV5 stability during MD production run.

Time evolution of (**a**) RMSD of Cα-atoms of TM helices S1 to S6 (blue) and all Cα atoms of the TRPV5 tetramer (red) bound to R-econazole, and (**b**) Cα RMSF for each monomer during the 25 ns production run of the TRPV5 complex bound to R-econazole. Panels **c** and **d** show the time evolution of RMSD and RMSF values for the TRPV5 complex bound to S-econazole.

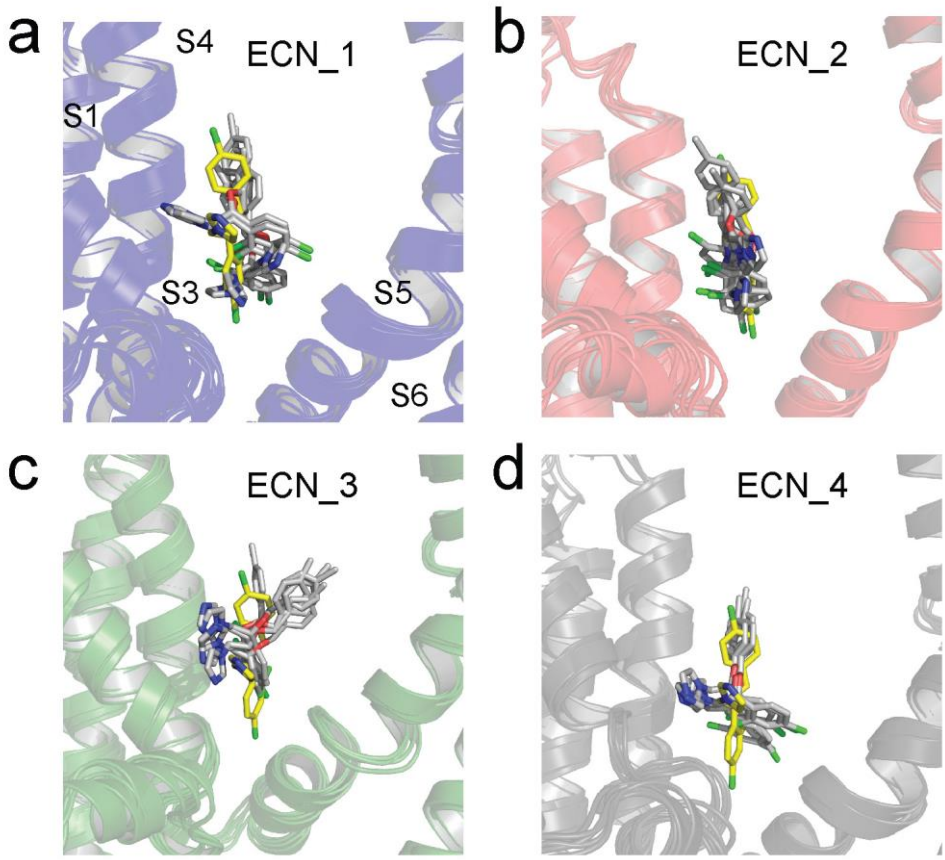

Supplementary Figure 10

Flexibility of econazole molecules during MD production run.

Binding modes of four R-econazole molecules (grey carbons; labeled ECN_1 to ECN_4 in panels (**a** to **d**) sampled during the 25 ns production run and compared to the initial manually docked pose of R-econazole (yellow carbons) into the assigned electron density. Each panel **a** to **d** shows five conformations of R-econazole within the four monomers of TRPV5 (monomers A to D colored blue, red, green, and dark grey, respectively) at simulation times 5 ns, 10 ns, 15 ns, 20 ns, and 25 ns.

Supplementary Table 1. Distances between econazole and the cryo-EM-inferred binding pocket residues of TRPV5. Those that remained within 4.0 Å from at least three of the four econazole molecules in either enantiomeric form during MD simulations are in bold. Distances reported are between heavy atoms of econazole and side chain heavy atoms of TRV5 residues. Error bars correspond to standard deviation of distance values sampled during simulation (n=2500).

Econazole S-enantiomer						**Econazole R-enantiomer**					
	Minimum Distance (Å) in docked structure	**Average minimum distance (Å) during MD**					**Minimum Distance (Å) in docked structure**	**Average minimum distance (Å) during MD**			
Residues		**ECN1**	**ECN2**	**ECN3**	**ECN4**	**Residues**		**ECN1**	**ECN2**	**ECN3**	**ECN4**
F425	3.4	4.4 ± 0.9	3.8 ± 0.3	3.6 ± 0.3	3.7 ± 0.3	**F425**	2.8	5.8 ± 1.4	3.9 ± 0.4	4.9 ± 0.7	4.0 ± 0.5
I428	3.4	3.9 ± 0.4	3.7 ± 0.2	3.7 ± 0.2	3.9 ± 0.3	**I428**	4.2	3.9 ± 0.3	3.9 ± 0.3	3.6 ± 0.2	3.7 ± 0.3
F456	7.7	6.7 ± 2.0	4.3 ± 0.8	7.2 ± 1.0	4.0 ± 0.4	F456	2.4	4.2 ± 0.6	4.2 ± 0.7	5.2 ± 1.7	3.9 ± 0.4
L460	3.5	6.0 ± 1.5	4.0 ± 0.5	4.2 ± 0.5	3.9 ± 0.4	**L460**	2.1	3.8 ± 0.5	3.8 ± 0.3	3.8 ± 0.3	3.7 ± 0.2
C463	3.9	4.6 ± 0.9	3.8 ± 0.3	3.7 ± 0.3	4.1 ± 0.4	**C463**	4.4	3.8 ± 0.3	4.0 ± 0.4	3.8 ± 0.3	3.7 ± 0.3
M466	4.0	5.2 ± 1.5	4.3 ± 0.7	4.8 ± 0.9	3.7 ± 0.3	M466	5.0	5.2 ± 1.5	4.0 ± 0.5	5.2 ± 1.1	4.7 ± 0.8
I482	3.8	4.7 ± 1.0	3.8 ± 0.3	4.2 ± 0.5	4.1 ± 0.4	I482	3.8	5.3 ± 1.5	7.1 ± 1.2	4.0 ± 0.5	5.0 ± 1.0
I486	4.0	3.7 ± 0.2	3.7 ± 0.3	3.8 ± 0.2	3.8 ± 0.3	**I486**	5.8	3.9 ± 0.4	4.6 ± 0.6	3.9 ± 0.3	3.7 ± 0.2
I564	4.0	5.5 ± 1.6	8.7 ± 0.7	8.6 ± 0.6	7.8 ± 0.6	I564	5.7	6.3 ± 1.6	11.0 ± 0.7	5.4 ± 1.9	5.8 ± 1.3
I565	3.6	4.0 ± 0.6	3.8 ± 0.4	4.0 ± 0.4	3.8 ± 0.3	**I565**	3.9	3.8 ± 0.3	6.9 ± 0.6	4.0 ± 0.5	3.8 ± 0.3